Published in final edited form as:
Circ Res. 2012 January 6; 110(1): 59–70. doi:10.1161/CIRCRESAHA.111.254672.

Adrenergic signaling controls RGK-dependent trafficking of cardiac voltage-gated L-type Ca^{2+} channels through PKD1

Bong Sook Jhun, PhD[#1], **Jin O-Uchi, MD, PhD**[#1], **Weiye Wang, PhD**[1], **Chang Hoon Ha, PhD**[1], **Jinjing Zhao, MD, PhD**[1], **Ji Young Kim, PhD**[1], **Chelsea Wong, MS**[1], **Robert T. Dirksen, PhD**[2], **Coeli M.B. Lopes, PhD**[#1,§], and **Zheng Gen Jin, PhD**[#1,§]

[1]Aab Cardiovascular Research Institute, Department of Medicine, University of Rochester School of Medicine and Dentistry, Rochester NY, 14642 USA.

[2]Department of Pharmacology and Physiology, University of Rochester School of Medicine and Dentistry, Rochester NY, 14642 USA.

[#] These authors contributed equally to this work.

Abstract

Rationale—The Rad-Gem/Kir-related family (RGKs) consists of small GTP-binding proteins that strongly inhibit the activity of voltage-gated calcium channels. Among RGKs, Rem1 is strongly and specifically expressed in cardiac tissue. However, the physiological role and regulation of RGKs, and Rem1 in particular, are largely unknown.

Objective—To determine if Rem1 function is physiologically regulated by adrenergic signaling, and thus, impacts voltage-gated L-type calcium channel (VLCC) activity in the heart.

Methods and Results—We found that activation of protein kinase D1 (PKD1), a protein kinase downstream of α_1-adrenergic signaling, leads to direct phosphorylation of Rem1, at Ser18. This results in an increase of the channel activity and plasma membrane expression, observed by using a combination of electrophysiology, live cell confocal microscopy and immunohistochemistry in heterologous expression system and neonatal cardiomyocytes. In addition, we show that stimulation of α_1-adrenergic receptor-PKD1-Rem1 signaling increases transverse-tubule (T-tubule) VLCC expression that results in increases L-type Ca^{2+} current density in adult ventricular myocytes.

Conclusion—α_1-adrenergic stimulation releases Rem1 inhibition of VLCCs through direct phosphorylation of Rem1 at Ser18 by PKD1, resulting in an increase of the channel activity and T-tubule expression. Our results uncover a novel molecular regulatory mechanism of VLCC

[§]Correspondence to: Zheng Gen Jin Phone: 585-275-3351, Fax: 585-276-9829 zheng-gen_jin@urmc.rochester.edu and Coeli MB Lopes Phone: 585-276-9784, Fax: 585-276-9829 coeli_lopes@urmc.rochester.edu.

Disclosures
None.

trafficking and function in the heart, and provide the first demonstration of physiological regulation of RGK function.

Keywords

Cav1.2; phenylephrine; adrenoceptor; patch clamp

Introduction

The voltage-gated calcium channels play a crucial role in regulating cellular excitability [1]. In cardiac muscle, Ca^{2+} influx through voltage-gated L-type calcium channels (VLCCs) regulates cardiac rhythm and controls muscle contractility by triggering Ca^{2+} release from the sarcoplasmic reticulum via excitation-contraction (E-C) coupling [2-4]. The alteration of VLCC density or function at the plasma membrane is a key regulator of Ca^{2+}-dependent cell signaling, gene expression and cell growth associated with a variety of cardiac diseases, including heart failure, ischemic heart dysfunction and cardiac arrhythmias, demonstrating a central role for post-translational modification of VLCC function in cardiac disease[5-9]. The VLCCs in the heart are multi-subunit transmembrane proteins (a pore-forming α_1-subunits, also named as Cav1.2, and auxiliary subunits, $\alpha_{2\delta}$ and β_{2a}) that open in response to membrane depolarization [1, 4]. VLCCs are particularly localized at sarcolemmal membrane structure called transverse tubular (T-tubule) system[10]. T-tubules occur at the Z line, at the end of each sarcomere and also show complex network of branching tubules with both transverse and longitudinal elements[10], which have crucial roles for the regulation of cardiac muscle contractility and rhythm [3, 4, 11, 12]. Although acute modulation of VLCCs by neurotransmitters such as adrenergic stimulation has been extensively studied [4, 11-15], surprisingly little is known about the molecular mechanisms underlying dynamic physiological and pathophysiological regulation of VLCC membrane expression by intracellular signal transduction.

Emerging evidence suggests that members of the RGK family (Rem1, Rem2, Rad, and Gem/Kir) strongly inhibit VLCC trafficking and activity when overexpressed in heterologous expression systems or native cells including heart, skeletal muscle and brain [16]. In particular,Rem1, a member of the RGK family, is abundantly expressed in the heart [17]. However, in native cells including cardiomyocytes, the physiological role of RGK proteins and their regulation by intracellular signaling are largely unknown.

Here we show that adrenergic stimulation releases Rem1 inhibition of VLCC. The release of Rem1-mediated VLCC inhibition in adult cardiomyocytes dramatically increases both T-tubule VLCC membrane expression and Ca^{2+} current density. We further show that adrenergic stimulation release of Rem1 inhibition of VLCC results from activation of protein kinase D1 (PKD1) [18, 19], a protein kinase downstream of α_1-adrenoceptor (α_1-AR) signaling, which phosphorylates Rem1 at Serine 18. Our results indicate that Rem1 phosphorylation at Serine 18 results in increased the Ca^{2+} current through VLCCs (I_{Ca}) due to increased VLCC plasma membrane expression. These findings uncover a novel molecular mechanism that modulates VLCC trafficking and function, and provides the first demonstration of physiological regulation of RGK function.

Material & Methods

An expanded Methods section is available in the Online Data Supplement.

Plasmid, Antibodies and Reagents

All plasmids, antibodies and reagents used for the experiments were shown in Online Data Supplement. Anti-phospho-Rem1(S18) was generated with a synthetic phosphopeptide corresponding to mouse Rem1 residues 12-24.

Cell Culture, Transfection and Infection

HEK293T cells and Hela cells were transfected with plasmids and used for experiments 24 hours after transfection. Neonatal and adult rat ventricular myocytes were isolated, cultured and infected with recombinant adenoviruses as previously described[20-22].

In Vitro Kinase Assays

Glutathione S-transferase (GST)-fusion protein expression plasmids for full-length WT Rem1 and Rem1 mutants were generated and used for *in vitro* kinase assays for PKD1[23].

Biochemistry

Whole cell lysates were used for Western blot and immunoprecipitation analyses[15, 24]. The expression level of $Ca_V1.2$ in the plasma membrane was determined by a cell-surface proteinbiotinylation assay[25].

Confocal Microscopy

Plasma membrane localization of $Ca_V1.2$ was quantified by line scan intensity measurements and reported as membrane/cytosol ratio (M/C ratio)[26]. Fast fourier transform (FFT) power spectra were used for quantification of T-tubular VLCC localization in adult cardiomyocytes[27].

Electrophysiology

Whole cell patch clamp experiments were conducted to measure I_{Ca} at room temperature (≈22°C) using extracellular solution containing 10 or 1 mmol/L Ca^{2+} in HEK293T cells[28] and cardiomyocytes[15], respectively.

Data and Statistical Analyses

All results are shown as mean ± standard error (SE). The number of the cells used for each analysis is shown in parentheses in the graphs. Unpaired Student's t-tests were performed when comparing two data sets. For multiple comparisons, a one-way ANOVA followed by posthoc Tukey test was performed. Statistical significance was set as a *P* value of <0.05.

Results

α_1-AR stimulation attenuates the inhibitory effect of Rem1 on VLCC function and plasma membrane expression

Rem1 is expressed in cardiomyocytes[16], but not endogenously expressed in HEK293T cells (online Figure I). To explore whether adrenergic signaling can release the inhibitory effects of Rem1 on I_{Ca}, we co-expressed VLCC subunits with Rem1 and adrenoceptors (ARs) (α_1- or β_1-AR) in HEK293T cells and determined the subcellular VLCC localization using confocal microscopy[26]. Cav1.2 (pore-forming α subunit), β_{2a} and $\alpha_{2\delta}$ subunits were co-transfected. Co-transfection of all 3 subunits resulted in the distinct expression of GFP-tagged $Ca_V1.2$ in the surface membrane (Figure 1A&B, online Figure II). As previously reported[29], without co-expression of β_{2a} subunits Cav1.2 was not expressed at the plasma membrane (online Figure II). In addition, co-expression of $\alpha_{2\delta}$ subunits increased the surface membrane expression level of $Ca_V1.2$- β_{2a} channels.

Rem1 co-expression caused $Ca_V1.2$ to be largely retained at the endoplasmic reticulum (ER) (Figure 1A&B, Figure 2A&B). Remarkably, the inhibitory effect of Rem1 on VLCC surface expression was dramatically attenuated by α_1-AR stimulation [10 μmol/L phenylephrine (Phe) for 2 hours] (Figure 1A&B), concomitant with $Ca_V1.2$ redistribution from the ER to the plasma membrane (Figure 2A&B). We determined the dose-dependence of 2hr-Phe treatment on Cav1.2 membrane expression, and found that 0.1 μmol/L Phe significantly increased channel membrane expression, with a maximal effect at 10 μmol/L (Online Figure III). The increase in VLCC surface expression by Phe was blocked by the α_1-AR antagonist prazosin (1 μmol/L) confirming that the effect is mediated through α_1-ARs (M/C ratio of Phe treated=0.93±0.29, n=13, untreated= 0.81±0.16, n=35, p=0.71). Acute α_1-AR stimulation (30sec-15min) did not significantly alter VLCC localization, but VLCCs gradually redistributed to the surface membrane after 1hr of stimulation (online Figure VI). In the absence of Rem1 expression, VLCC membrane expression was not enhanced by Phe stimulation (Online Figure II). Rem1-mediated reduction in $Ca_V1.2$ surface expression and relief by α_1-AR stimulation were also confirmed by a cell-surface protein biotinylation assay[25] (Online Figure V).

VLCCs function was estimated in whole-cell patch experiments. Consistent with reduction in surface membrane expression, Rem1 expression markedly decreased I_{Ca} as previously reported for Rem1 and other RGKs[16]. α_1-AR stimulation (10 μmol/L Phe for 2 hour) restored I_{Ca} magnitude to levels comparable to that observed in the absence of Rem1 without altering the voltage dependence of channel activation (Figure 1D, Online Table. I). Acute activation of α_1-AR signaling did not activate I_{Ca} both in the presence and absence of Rem1 in this cell line (Online Figure VI). In order to functionally assess the plasma membrane expression level of the channels under these conditions, we activated channels with the Ca^{2+} channel agonist Bay K 8644 (BayK) [22]. In control cells, I_{Ca} was significantly increased (Online Figure VII) as previously reported[22] by BayK treatment. In Rem1-transfected cells, I_{Ca} was also significantly increased by BayK treatment. However, the average fold increase in I_{Ca} is the same among these three groups and I_{Ca} in Rem1-transfected cells still remained at lower level than those observed in the absence of Rem1 or

in the presence of Rem1 after Phe stimulation (Online Figure VII). These results indicate that I_{Ca} inhibition by Rem1 under these conditions is mainly due to a decrease in VLCC plasma membrane expression, which can be released by α_1-AR stimulation.

To explore whether β_1-adrenergic signaling can also release the inhibitory effects of Rem1 on I_{Ca}, we co-expressed VLCC subunits with Rem1 and β_1-ARs in HEK293Tcells. However, the inhibitory effect of Rem1 on VLCC trafficking was not reversed by β_1-AR stimulation (100 nμmol/L isoproterenol for 2 hours) in these experiments (Online Figure VIII). Because β_1-AR show agonist-induced internalization during long-term agonist stimulation, not observed with α_{1A}-AR (online Figure IX), we also used a direct adenylyl cyclase activator (1 μmol/L forskolin for 2 hours) to directly activate downstream β_1-AR signaling. The inhibitory effect of Rem1 on VLCC trafficking was also not reversed by forskolin applications (Online Figure VIII), indicating that release of Rem1 inhibition on I_{Ca} is specific to α_1-AR signaling.

α_1-AR stimulation regulates VLCC function and plasma membrane expression through PKD1-mediated phosphorylation of Rem1 at Ser18

PKD1 is a newly described serine/threonine protein kinase involved in α_1-AR signaling that plays important roles in the cardiovascular system[18, 19]. Ser18 of Rem1 lies within a PKD consensus motif LXRXX(T*/S*) (Figure 3A)[18, 19] conserved across multiple eukaryotic Rem1 species (Online Figure X). The amino acid sequence surrounding Ser 290 of Rem1 is also closely related to the PKD consensus motif (Figure 3A). To examine whether PKD1 could phosphorylate Rem1 at either of these potential sites, we performed *in vitro* kinase assays using GST-fusion proteins and found that Ser18 (but not Ser290) is a PKD1-specific phosphorylation site in Rem1 (Figure 3B). We further demonstrated that PKD1 phosphorylates Rem1-Ser18 *in situ* (Figure 3C) using a custom-made antibody (see also Online Figure XI). Moreover, PKD1 interacted with Rem1 and this interaction increased when PKD1 was activated (Online Figure XII). To test whether α_1-AR signaling phosphorylates Rem1-Ser18 through PKD1 activation, we co-transfected α_1-AR and Rem1 into HEK293T cells and stimulated the cells with phenylephrine. In un-stimulated cells a low-level Rem1 phosphorylation was observed, suggesting that PKD signaling has some activity under basal conditions (Figure 3D). Phosphorylation of Rem1-Ser18 was increased within 30-sec of Phe stimulation, concomitant with endogenous PKD1 activation and this effect remained for up to 2 hrs (Figure 3D, Online Figure XIII). Rem1 phosphorylation was also observed with stimulation by lower concentrations of phenylephrine of Phe (0.1 μmol/L) (Online Figure XIV). Increased Rem1-Ser18 phosphorylation by Phe was blocked by the pretreatment with 1 μmol/L prazosin (Online Figure XV). In addition, PKD1 activation, as observed after α_1-AR stimulation, promoted $Ca_V1.2$ redistribution from the ER to the surface membrane (Figures 4A). Expression of the Rem1-Ser18Ala mutant (Rem1SA) abolished the α_1-AR- and PKD1-mediated inhibitory regulation of I_{Ca} and $Ca_V1.2$ trafficking to the surface membrane (Figure 4B). Similarly, co-expression of a kinase-negative PKD1 mutant (PKD-KN) reduced the phosphorylation of Rem1 and abolished rescue of I_{Ca} produced by Phe (Online Figure XVI). Results from direct cell application of a PKC activator and cAMP analog demonstrated that PKD1 activation and Rem1 phosphorylation occurs downstream of PKC but not cAMP (Online Figure VIII).

Collectively, these results indicated that PKD1 directly phosphorylates Rem1-Ser18 upon α_1-AR stimulation, promoting VLCC plasma membrane localization, and thus, increasing I_{Ca}. Rem1-Ser18 is a potential phosphorylation site suggested to be required for the binding RGKs to the scaffolding protein 14-3-3 *in vitro*, which is thought to regulate subcellular RGK localization [16]. However, the upstream signaling pathway that controls RGK phosphorylation remains unknown. We found that Ser18 phosphorylation promotes Rem1 binding to 14-3-3 (Online Figure XVII) and translocation to the nucleus (Online Figure XVIII), suggesting that Ser18 phosphorylation increases the ability of 14-3-3 to recruit Rem1, thereby interfering with the ability of Rem1 to associate with VLCC and inhibit VLCC surface membrane trafficking and function. Rem1 in unstimulated cells strongly co-localized with the ER marker, consistent with the role of Rem1 in suppressing VLCC membrane expression.

α_1-AR stimulation enhances VLCC expression at the plasma membrane through PKD1-dependent phosphorylation of Rem1 at Ser18 in neonatal cardiomyocytes

Our results indicate that α_1-AR stimulation results in PKD1-mediated phosphorylation of Rem1 at Ser18 and a subsequent increase in VLCC surface membrane expression and function following heterologous expression in HEK293T cells. Next we investigated the role of the proposed α_1-AR-PKD1-Rem1-LVCC signaling pathway in native cardiomyocytes. We found that Rem1 is expressed in whole-cell lysates of neonatal rat ventricular myocytes and that α_1-AR stimulation by Phe (30 min) promoted PKD1 activation and Rem1 phosphorylation at Ser18 (Online Figure XIX). In addition, we determined the subcellular localization of VLCC in neonatal cardiomyocytes before and after α_1-AR stimulation by Phe using an anti-$Ca_V1.2$ antibody (Figure 5, Online Figure XX). In agreement to previous reports, [11, 30] $Ca_V1.2$ labeling was observed both at the surface membrane and intracellularly under basal conditions (Online Figure XX). After α_1-AR stimulation (10 μμmol/L Phe for 2 hours), $Ca_V1.2$ was preferentially localized at the plasma membrane with additional nuclear punctuate staining (Figure 5A, Online Figure XX) presumably due to the stimulation of endogenous Rem1. M/C ratio was significantly increased by Phe stimulation (Figure 5A &C, Online Figure XX). To confirm the involvement of PKD1 activity in this effect, myocytes were infected with GFP-tagged PKD-KN and cellular localization of $Ca_V1.2$ was determined before and after α_1-AR stimulation. GFP infection alone did not alter $Ca_V1.2$ localization either before or after Phe treatment (compare with Figure 5A, Online Figure XX). However, PKD-KN-infected myocytes did not show a significant increase in $Ca_V1.2$ plasma membrane expression in response to Phe (Figure 5B&C). These results demonstrate that α_1-AR stimulation induces an increase of VLCC surface membrane expression through a PKD1-dependent mechanism in neonatal cardiomyocytes. To confirm the involvement of Rem1 phosphorylation at Ser18 in this process, myc-tagged WT-Rem1 or Rem1-S18A was overexpressed by adenoviral infection and the subcellular localization of $Ca_V1.2$ was assessed before and after α_1-AR stimulation (Figure 5D to F). Overexpression of both WT-Rem1 (M/C ratio=0.93±0.15, n=9) and Rem1-S18A (M/C ratio=0.88±0.09, n=10) significantly decreased the M/C ratio compared to control (LacZ-infected cells, M/C ratio=1.63 0.24, n=11) (P=0.03 and 0.01, respectively). In WT-Rem1-expressing cells, Phe stimulation promoted $Ca_V1.2$ redistribution to the plasma membrane and significantly reduced the degree of co-localization with Rem1 (Figure 5D&F, Online Figure XXI).

However, in Rem1-S18A-infected myocytes, Phe stimulation did not alter $Ca_V1.2$ subcellular localization or Rem1-$Ca_V1.2$ co-localization (Figure 5E&F, Online Figure XXI). These results indicate that α_1-AR stimulation increases VLCC membrane expression in neonatal cardiomyocytes through PKD-dependent phosphorylation of Rem1 at Ser18.

α_1-AR stimulation enhances T-tubule VLCC expression in adult ventricular myocytes through PKD1-dependent phosphorylation of Rem1 at Ser18

We next investigated the role of the α_1-AR-PKD1-Rem1-VLCC signaling pathway in the heart by measuring $Ca_v1.2$ localization and I_{Ca} function in adult rat ventricular myocytes in response to sustained α_1-AR stimulation. By using the plasma membrane marker Wheat Germ Agglutinin (WGA), we confirmed that the cellular morphology, T-tubule structure and its periodicity (~1.8 μm) [10] were preserved in our cultured myocytes up to ≈40hr after infection (Figure 6A&D, Online Figure XXII and XXIII).

We measured the effect of Rem1 and Rem1(S18A) overexpression and α_1-AR stimulation on $Ca_v1.2$ localization and I_{Ca} in adult cardiomyocyes. We used fast fourier transform (FFT) power spectral analysis of $Ca_V1.2$ immunoflurescence to quantify VLCC T-tubular localization[27]. In WT-Rem1-overexpressing myocytes, α_1-AR stimulation promoted Rem1 phosphorylation, $Ca_V1.2$ T-tubule redistribution, and partially recovered I_{Ca} without changes in Cav1.2 protein expression (Figure 6A to C, Online Figure XXV). Rem1 co-localized well with T-tubule $Ca_V1.2$ channels before, but not after Phe stimulation (Online Figure XXVI). In Rem1-S18A-overexpressing adult ventricular myocytes, α_1-AR-mediated regulation of VLCC T-tubule expression and I_{Ca} activation were not observed (Figure 6D to F). These results indicate that α_1-AR stimulation increases both VLCC function and T-tubule localization in adult cardiomyocytes through PKD-dependent phosphorylation of Rem1 at Ser18. All experiments were measured 40 hours after Rem1 adenovirus infection, the effects of Rem1 overexpression on channel membrane localization were not observed 24 hours after infection with WT-Rem1 adenovirus (Online Figure XXV), although cells expressed ≈4-5 times more Rem1 compared to endogenous Rem1 expression, consistent with the slow turn-over observed for the Cav1.2 protein[31]. Forty hours after infection with WT-Rem1 adenovirus, myocytes expressed ≈8-10 times more Rem1 compared endogenous Rem1 (Online Figure XXV).

To determine whether PKD1 activation could regulate VLCC without overexpression of Rem1, presumably by regulating endogenous Rem1, we measure the effect of α_1-AR stimulation (10 μμmol/L Phe for 2 hours) on VLCC T-tubular distribution and current. Phe treatment increased I_{Ca} in both freshly isolated and cultured adult ventricular myocytes (Online Figures XXIII, XXIV). Cultured cardiomyocytes were infected with Lac-Z as control for Rem1 infected cells. VLCC T-tubular distribution was increased after Phe application without changing total the Cav1.2 expression levels (Online Figure XXIII & XXV). T-tubular redistribution of $Ca_V1.2$ induced by α_1-AR stimulation was abolished by infection with PKD-KN (online figure XXVI).

Discussion

In the present study, we characterize a novel molecular mechanism for the regulation of VLCC cell-surface expression. We show that PKD1 induces an increase in cell surface VLCC density through phosphorylation of small GTP-binding protein Rem1 in response to α_1-AR stimulation, leading to a subsequent increase in Ca^{2+} channel activity (Figure 7). Our study demonstrates that Rem1 is a PKD1 substrate and that a novel α_1-AR-PKD1-Rem1 signaling pathway dynamically regulates VLCC function in cardiomyocytes. In particular, in adult ventricular myocytes, adrenergic stimulation releases Rem1 inhibition of VLCCs, resulting in an increase in channel activity and expression at T-tubules. T-tubule localization of VLCCs is key to the control cardiac excitability and contractility[3, 4, 11, 12]. Our results uncover a novel molecular regulatory mechanism of VLCC trafficking and function, and provide the first demonstration of physiological regulation of RGK function.

Previous reports proposed that RGK-mediated Ca^{2+}-current suppression in heterologous expression systems results from either: 1) a decrease the number of pore subunits of Ca^{2+} channels expressed at the plasma membrane [32-36] or 2) inhibition of surface membrane channel activity [22, 22, 35, 37, 38]. Our data agrees with Rem1 decreasing VLCC expression at plasma membrane in both a heterologous expression system and in native cardiomyocytes. Moreover, changes in VLCC membrane localization correlated well with the functional effects observed. Our data suggest that while short term expression of Rem1 may inhibits channel activity without decreasing membrane expression, longer term Rem1 expression leads to a decrease in channel membrane levels. This is consistent with the slow turn over observed for this channel[16] and suggests that Rem1 may decrease channel insertion into the plasma membrane. Interestingly, the PKD1-Rem1(S18)-mediated increase in membrane expression is observed after only one hour persistent activation of the signaling, suggesting that PKD1-Rem1 signaling can release a ‘VLCC-reserve’ that would help maintain VLCC activity at persistently high adrenergic states. Taken together our data indicate channel trafficking to be a major contributor to PKD1-Rem1 regulation of VLCC in cardiomyocytes.

Our data would also suggest that the increase in VLCC membrane expression through α_1-AR-PKD1-Rem1 signaling could contribute to the cytosolic Ca^2 overload when catecholamine levels are chronically and strongly increased under pathophysiological stress conditions such as cardiac hypertrophy and heart failure. However, potential limitations of the present study include the alteration in integrity of plasma and intracellular membrane systems such as T-tubules and ER membranes in isolated cardiomyocytes after culture and 2hr-Phe treatment. Further investigation would be needed to clarify the detailed mechanism and the role of endogenous expression levels of Rem1 in the regulation of VLCC membrane expression by α_1-AR-PKD1 signaling in cardiomyocytes and *in vivo* under the physiological conditions.

Among RGKs, both Rem1 and Rad are expressed at significant mRNA and protein levels in the heart [16] and are thought to regulate VLCC function [22, 35, 39, 40]. Although Ser18 is conserved in both proteins[16], it is not part of a PKD1 substrate motif in Rad. However, further investigation would be needed to clarify the involvement of Rad in the regulation of VLCC by α_1-AR-PKD1 signaling in cardiomyocytes. Changes in ER morphology in Rem1-

overexpressing cells were observed (Figures 1 and 2), possibly due to the Rem1 regulation of cytoskeleton dynamics as has been reported for other RGKs[16]. While morphological remodeling of the ER by Rem1 might contribute to Rem1-mediated inhibition of VLCC trafficking, further studies are needed to more precisely define the underlying mechanism.

In conclusion, we provide the first evidence for a receptor-mediated signaling pathway that can dynamically regulate Rem1 inhibition of VLCCs (Figure 7) in cardiovascular system. Specifically, we show that α_1-AR-PKD1-mediated phosphorylation of Rem1-S18 dramatically attenuates Rem1 suppression of VLCC membrane expression and function by promoting the association of Rem1 with 14-3-3 and consequently by reducing the co-localization of Rem1 and VLCCs. Because alterations in VLCC T-tubular membrane expression and function are implicated in cardiovascular disease[7, 11, 12, 27], the PKD1-Rem1-VLCCs regulatory pathway will provide the new insight to understanding cardiac E-C coupling regulation and also will open new therapeutic perspectives for cardiac hypertrophy, heart failure and arrhythmias.

Supplementary Material

Refer to Web version on PubMed Central for supplementary material.

Acknowledgments

We are gratefully thanks for Ms. Jaime Sorenson, Dr. Elena Fujiwara, Ms. Mehreen Butt and Mr. Michael Cypress for their technical assistance.

Source of Funding

This work was supported by NIH grants HL80611 (to Z.G.J.), AR44657 (to R.T.D.), an American Heart Association (AHA) Predoctoral Fellowship (to W.W.), AHA Postdoctoral Fellowships (to J. O.-U. and C. H. H.), a Foreign Study Grant Award of Kanae Foundation (to J. O.-U.) and a Irisawa Memorial Promotion Award for Young Physiologists (to J. O.-U.).

Non-standard Abbreviations and Acronyms

RGK	Rad-Gem/Kir-related family
VLCC	voltage-gated L-type calcium channels
PKD1	protein kinase D1
T-tubules	transverse tubules
AR	adrenoceptor
I_{Ca}	the Ca^{2+} current through VLCCs
GST	Glutathione S-transferase
M/C ratio	membrane/cytosol ratio
FFT	Fast Fourier Transform
WGA	Wheat Germ Agglutinin
Phe	phenylephrine

PKD-SE	Constitutive active PKD1
PKD-KN	kinase-negative PKD1 mutant
BayK	Bay K 8644

Reference List

1. Dai S, Hall DD, Hell JW. Supramolecular assemblies and localized regulation of voltage-gated ion channels. Physiol Rev. 2009; 89:411–52. [PubMed: 19342611]
2. Benitah JP, Alvarez JL, Gomez AM. L-type Ca(2+) current in ventricular cardiomyocytes. J Mol Cell Cardiol. 2010; 48:26–36. [PubMed: 19660468]
3. Bers DM. Cardiac excitation-contraction coupling. Nature. 2002; 415:198–205. [PubMed: 11805843]
4. Kamp TJ, Hell JW. Regulation of cardiac L-type calcium channels by protein kinase A and protein kinase C. Circ Res. 2000; 87:1095–102. [PubMed: 11110765]
5. Gaur N, Rudy Y, Hool L. Contributions of ion channel currents to ventricular action potential changes and induction of early afterdepolarizations during acute hypoxia. Circ Res. 2009; 105:1196–203. [PubMed: 19875728]
6. Kubalova Z, Terentyev D, Viatchenko-Karpinski S, Nishijima Y, Gyorke I, Terentyeva R, da Cunha DN, Sridhar A, Feldman DS, Hamlin RL, Carnes CA, Gyorke S. Abnormal intrastore calcium signaling in chronic heart failure. Proc Natl Acad Sci U S A. 2005; 102:14104–9. [PubMed: 16172392]
7. Song LS, Sobie EA, McCulle S, Lederer WJ, Balke CW, Cheng H. Orphaned ryanodine receptors in the failing heart. Proc Natl Acad Sci U S A. 2006; 103:4305–10. [PubMed: 16537526]
8. Boixel C, Gonzalez W, Louedec L, Hatem SN. Mechanisms of L-type Ca(2+) current downregulation in rat atrial myocytes during heart failure. Circ Res. 2001; 89:607–13. [PubMed: 11577026]
9. Chen X, Nakayama H, Zhang X, Ai X, Harris DM, Tang M, Zhang H, Szeto C, Stockbower K, Berretta RM, Eckhart AD, Koch WJ, Molkentin JD, Houser SR. Calcium influx through Cav1.2 is a proximal signal for pathological cardiomyocyte hypertrophy. J Mol Cell Cardiol. 2011; 50:460–70. [PubMed: 21111744]
10. Brette F, Orchard C. T-tubule function in mammalian cardiac myocytes. Circ Res. 2003; 92:1182–92. [PubMed: 12805236]
11. Balijepalli RC, Foell JD, Hall DD, Hell JW, Kamp TJ. Localization of cardiac L-type Ca(2+) channels to a caveolar macromolecular signaling complex is required for beta(2)-adrenergic regulation. Proc Natl Acad Sci U S A. 2006; 103:7500–5. [PubMed: 16648270]
12. Brette F, Rodriguez P, Komukai K, Colyer J, Orchard CH. beta-adrenergic stimulation restores the Ca transient of ventricular myocytes lacking t-tubules. J Mol Cell Cardiol. 2004; 36:265–75. [PubMed: 14871554]
13. Dai S, Hall DD, Hell JW. Supramolecular assemblies and localized regulation of voltage-gated ion channels. Physiol Rev. 2009; 89:411–52. [PubMed: 19342611]
14. Boutjdir M, Restivo M, Wei Y, El-Sherif N. Alpha 1- and beta-adrenergic interactions on L-type calcium current in cardiac myocytes. Pflugers Arch. 1992; 421:397–9. [PubMed: 1357626]
15. O-Uchi J, Sasaki H, Morimoto S, Kusakari Y, Shinji H, Obata T, Hongo K, Komukai K, Kurihara S. Interaction of alpha1-adrenoceptor subtypes with different G proteins induces opposite effects on cardiac L-type Ca2+ channel. Circ Res. 2008; 102:1378–88. [PubMed: 18467629]
16. Correll RN, Pang C, Niedowicz DM, Finlin BS, Andres DA. The RGK family of GTP-binding proteins: regulators of voltage-dependent calcium channels and cytoskeleton remodeling. Cell Signal. 2008; 20:292–300. [PubMed: 18042346]
17. Finlin BS, Andres DA. Rem is a new member of the Rad- and Gem/Kir Ras-related GTP-binding protein family repressed by lipopolysaccharide stimulation. J Biol Chem. 1997; 272:21982–8. [PubMed: 9268335]

18. Ha CH, Jin ZG. Protein kinase D1, a new molecular player in VEGF signaling and angiogenesis. Mol Cells. 2009; 28:1–5. [PubMed: 19655095]
19. Avkiran M, Rowland AJ, Cuello F, Haworth RS. Protein kinase d in the cardiovascular system: emerging roles in health and disease. Circ Res. 2008; 102:157–63. [PubMed: 18239146]
20. Kang M, Walker JW. Protein kinase C delta and epsilon mediate positive inotropy in adult ventricular myocytes. J Mol Cell Cardiol. 2005; 38:753–64. [PubMed: 15850569]
21. Xu X, Colecraft HM. Primary culture of adult rat heart myocytes. J Vis Exp. 2009; (28)
22. Xu X, Marx SO, Colecraft HM. Molecular mechanisms, and selective pharmacological rescue, of Rem-inhibited CaV1.2 channels in heart. Circ Res. 2010; 107:620–30. [PubMed: 20616312]
23. Hausser A, Storz P, Link G, Stoll H, Liu YC, Altman A, Pfizenmaier K, Johannes FJ. Protein kinase C mu is negatively regulated by 14-3-3 signal transduction proteins. J Biol Chem. 1999; 274:9258–64. [PubMed: 10092600]
24. Ha CH, Wang W, Jhun BS, Wong C, Hausser A, Pfizenmaier K, McKinsey TA, Olson EN, Jin ZG. Protein kinase D-dependent phosphorylation and nuclear export of histone deacetylase 5 mediates vascular endothelial growth factor-induced gene expression and angiogenesis. J Biol Chem. 2008; 283:14590–9. [PubMed: 18332134]
25. Jiang M, Xu X, Wang Y, Toyoda F, Liu XS, Zhang M, Robinson RB, Tseng GN. Dynamic partnership between KCNQ1 and KCNE1 and influence on cardiac IKs current amplitude by KCNE2. J Biol Chem. June 12. 2009; 284(24):16452–62. [PubMed: 19372218]
26. Williams DM, Lopes CM, Rosenhouse-Dantsker A, Connelly HL, Matavel A, Uchi J, McBeath E, Gray DA. Molecular basis of decreased Kir4.1 function in SeSAME/EAST syndrome. J Am Soc Nephrol. 2010; 21:2117–29. [PubMed: 21088294]
27. Wei S, Guo A, Chen B, Kutschke W, Xie YP, Zimmerman K, Weiss RM, Anderson ME, Cheng H, Song LS. T-tubule remodeling during transition from hypertrophy to heart failure. Circ Res. 2010; 107:520–31. [PubMed: 20576937]
28. Fallon JL, Baker MR, Xiong L, Loy RE, Yang G, Dirksen RT, Hamilton SL, Quiocho FA. Crystal structure of dimeric cardiac L-type calcium channel regulatory domains bridged by Ca2+* calmodulins. Proc Natl Acad Sci U S A. 2009; 106:5135–40. [PubMed: 19279214]
29. Chien AJ, Zhao X, Shirokov RE, Puri TS, Chang CF, Sun D, Rios E, Hosey MM. Roles of a membrane-localized beta subunit in the formation and targeting of functional L-type Ca2+ channels. J Biol Chem. 1995; 270:30036–44. [PubMed: 8530407]
30. Seki S, Nagashima M, Yamada Y, Tsutsuura M, Kobayashi T, Namiki A, Tohse N. Fetal and postnatal development of Ca2+ transients and Ca2+ sparks in rat cardiomyocytes. Cardiovasc Res. 2003; 58:535–48. [PubMed: 12798426]
31. Catalucci D, Zhang DH, Desantiago J, Aimond F, Barbara G, Chemin J, Bonci D, Picht E, Rusconi F, Dalton ND, Peterson KL, Richard S, Bers DM, Brown JH, Condorelli G. Akt regulates L-type Ca2+ channel activity by modulating Cavalpha1 protein stability. J Cell Biol. 2009; 184:923–33. [PubMed: 19307602]
32. Bannister RA, Colecraft HM, Beam KG. Rem inhibits skeletal muscle EC coupling by reducing the number of functional L-type Ca2+ channels. Biophys J. 2008; 94:2631–8. [PubMed: 18192376]
33. Beguin P, Mahalakshmi RN, Nagashima K, Cher DH, Ikeda H, Yamada Y, Seino Y, Hunziker W. Nuclear sequestration of beta-subunits by Rad and Rem is controlled by 14-3-3 and calmodulin and reveals a novel mechanism for Ca2+ channel regulation. J Mol Biol. 2006; 355:34–46. [PubMed: 16298391]
34. Beguin P, Nagashima K, Gonoi T, Shibasaki T, Takahashi K, Kashima Y, Ozaki N, Geering K, Iwanaga T, Seino S. Regulation of Ca2+ channel expression at the cell surface by the small G-protein kir/Gem. Nature. 2001; 411:701–6. [PubMed: 11395774]
35. Yang T, Xu X, Kernan T, Wu V, Colecraft HM. Rem, a member of the RGK GTPases, inhibits recombinant CaV1.2 channels using multiple mechanisms that require distinct conformations of the GTPase. J Physiol. 2010; 588:1665–81. [PubMed: 20308247]
36. Sasaki T, Shibasaki T, Beguin P, Nagashima K, Miyazaki M, Seino S. Direct inhibition of the interaction between alpha-interaction domain and beta-interaction domain of voltage-dependent Ca2+ channels by Gem. J Biol Chem. 2005; 280:9308–12. [PubMed: 15615719]

37. Chen H, Puhl HL III, Niu SL, Mitchell DC, Ikeda SR. Expression of Rem2, an RGK family small GTPase, reduces N-type calcium current without affecting channel surface density. J Neurosci. 2005; 25:9762–72. [PubMed: 16237180]

38. Crump SM, Correll RN, Schroder EA, Lester WC, Finlin BS, Andres DA, Satin J. L-type calcium channel alpha-subunit and protein kinase inhibitors modulate Rem-mediated regulation of current. Am J Physiol Heart Circ Physiol. 2006; 291:H1959–H1971. [PubMed: 16648185]

39. Wang G, Zhu X, Xie W, Han P, Li K, Sun Z, Wang Y, Chen C, Song R, Cao C, Zhang J, Wu C, Liu J, Cheng H. Rad as a novel regulator of excitation-contraction coupling and beta-adrenergic signaling in heart. Circ Res. 2010; 106:317–27. [PubMed: 19926875]

40. Yada H, Murata M, Shimoda K, Yuasa S, Kawaguchi H, Ieda M, Adachi T, Murata M, Ogawa S, Fukuda K. Dominant negative suppression of Rad leads to QT prolongation and causes ventricular arrhythmias via modulation of L-type Ca2+ channels in the heart. Circ Res. 2007; 101:69–77. [PubMed: 17525370]

Novelty and Significance

What is known?

- RGK proteins are strong inhibitor of voltage-gated calcium channels.
- One of the RGKs, Rem1 is highly expressed in heart.
- The physiological role of Rem1 and its upstream regulation is unknown.

What new information does this article contribute?

- α-adrenergic receptor stimulation dramatically attenuates Rem1-mediated inhibition of VLCC function and promotes T-tubular localization in cardiomyocytes
- PKD1-dependent Rem1 phosphorylation of Rem1(S18) mediates the α-adrenergic regulation of VLCC.
- Stimulation of α-adrenergic-PKD1 and endogenous Rem1 signaling, regulates cardiac VLCC channels, demonstrating for the first time a physiological role of Rem1 in the heart.

Despite the widespread expression of small GTP-binding proteins (RGK), and their strong inhibition of VLCC in multiple tissues, the physiological regulation of RGK-mediated signaling remains elusive. In addition, despite the fact that PKD has been implicated in the regulation of diverse biological processes, only a few substrates are known. Here we show that Rem 1 is a novel PKD substrate and that adrenergic stimulation regulates plasma membrane expression of cardiac L-type calcium channels through PKD-dependent Rem1 phosphorylation. This work uncovers a novel molecular mechanism of modulation of voltage-gated calcium channel (VLCC) function and provides the first demonstration of physiologic regulation of the function of the small GTP-binding protein Rem1.

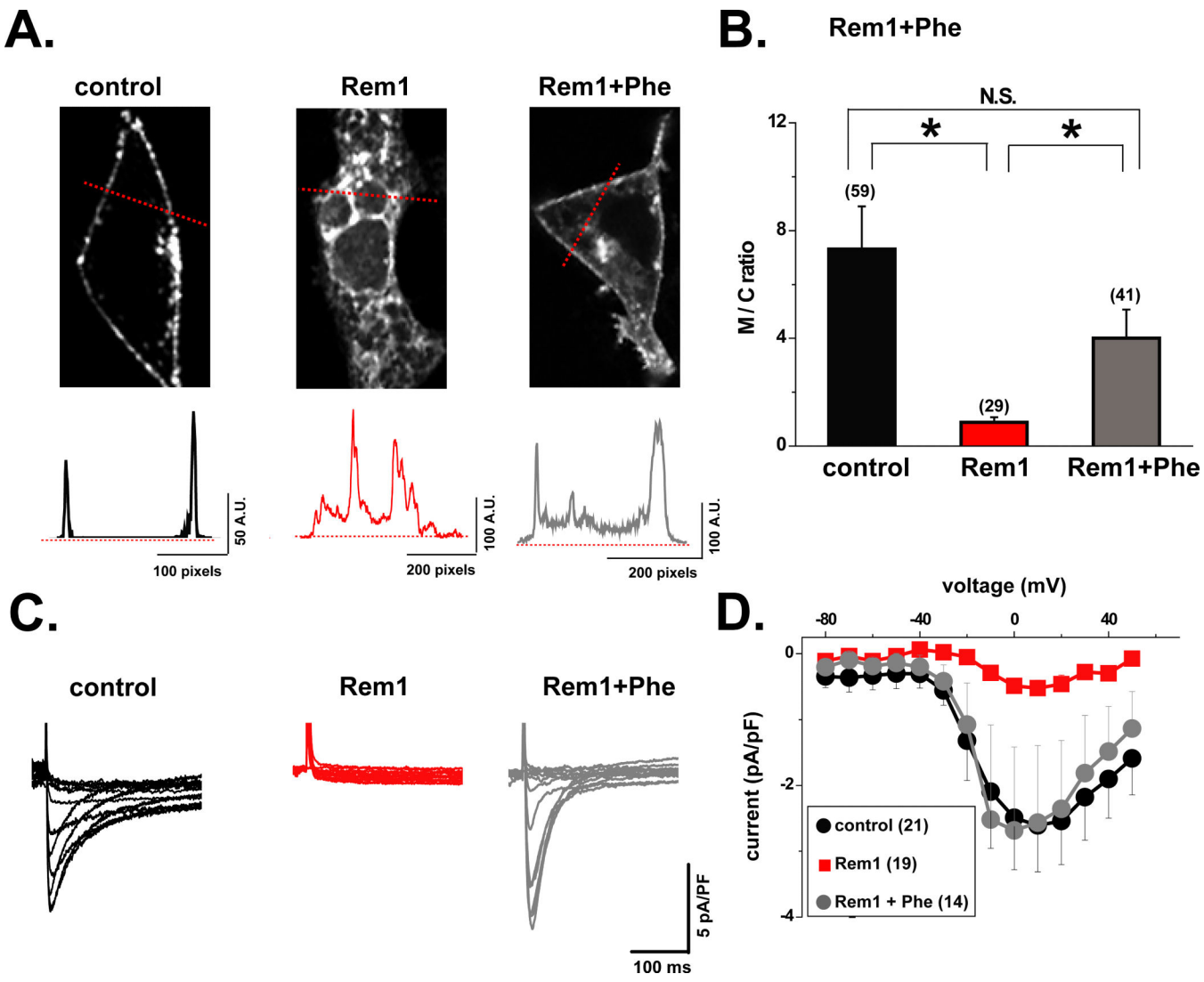

Figure 1. α_1-AR stimulation attenuates the inhibitory effect of Rem1 on VLCC function and surface-membrane expression

A. Subcellular localization of GFP-tagged $Ca_V1.2$. VLCC subunits and α_{1A}-AR were co-transfected with (middle, right) or without (left) WT-Rem1 in HEK293T cells. Rem1-transfected cells were also stimulated with 10 μmol/L Phe for 2 hours (right). GFP-emission profiles at a cross-section of the cells are shown below. A.U, fluorescence arbitrary units. **B.** Effect of Rem1 expression and Phe stimulation on VLCC localization. The ratio of fluorescence intensity at the surface membrane and cytosol was shown as M/C ratio (Online Figure XXVII). The number of the cells used for each condition is shown in parentheses. N.S., not significant. **C.** Effect of Rem1 expression and Phe stimulation on I_{Ca}. Representative family of I_{Ca} traces are obtained from the cells showing in panel A. **D.** Effect of Rem1 expression and Phe stimulation on current-voltage relationship of I_{Ca}.

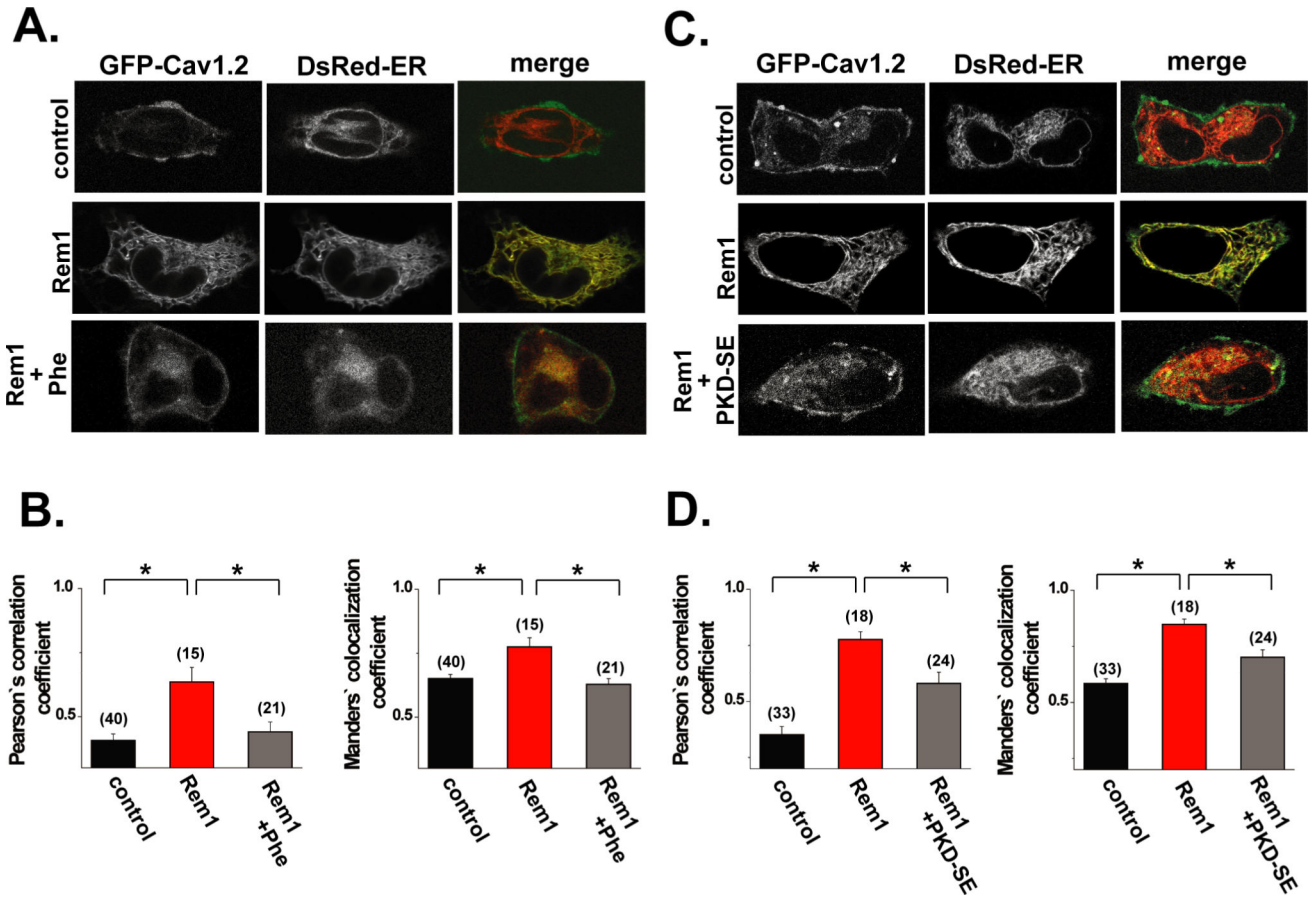

Figure 2. α_1-AR stimulation modulates subcellular localization of Ca^{2+} channel in Rem1-overexpressed HEK293Tcells through PKD1 activation

A. Representative confocal images of GFP-tagged Cav1.2 and Ds-Red ER marker co-localizations in Rem1 and α_{1A}-AR-overexpressed HEK293T cells with (Rem1+Phe, bottom panels) or without Phe stimulation (Rem1, middle panels) Rem1-transfected cells were stimulated with 10 μmol/L Phe for 2 hours. A cell without expression of Rem1 is shown as control (top panels). **B.** Summary data of quantitative colocalization analysis (see also Online Material and Methods). **C.** Representative confocal images of GFP-tagged Cav1.2 and Ds-Red ER marker co-localizations in Rem1-overexpressed HEK293T cells with (Rem1+PKD-SE, bottom panels) or without co-expression of PKD-SE (Rem1, middle panels). A cell without expression of both Rem1 and PKD-SE is shown as control (top panels). **D.** Summary data of quantitative colocalization analysis.

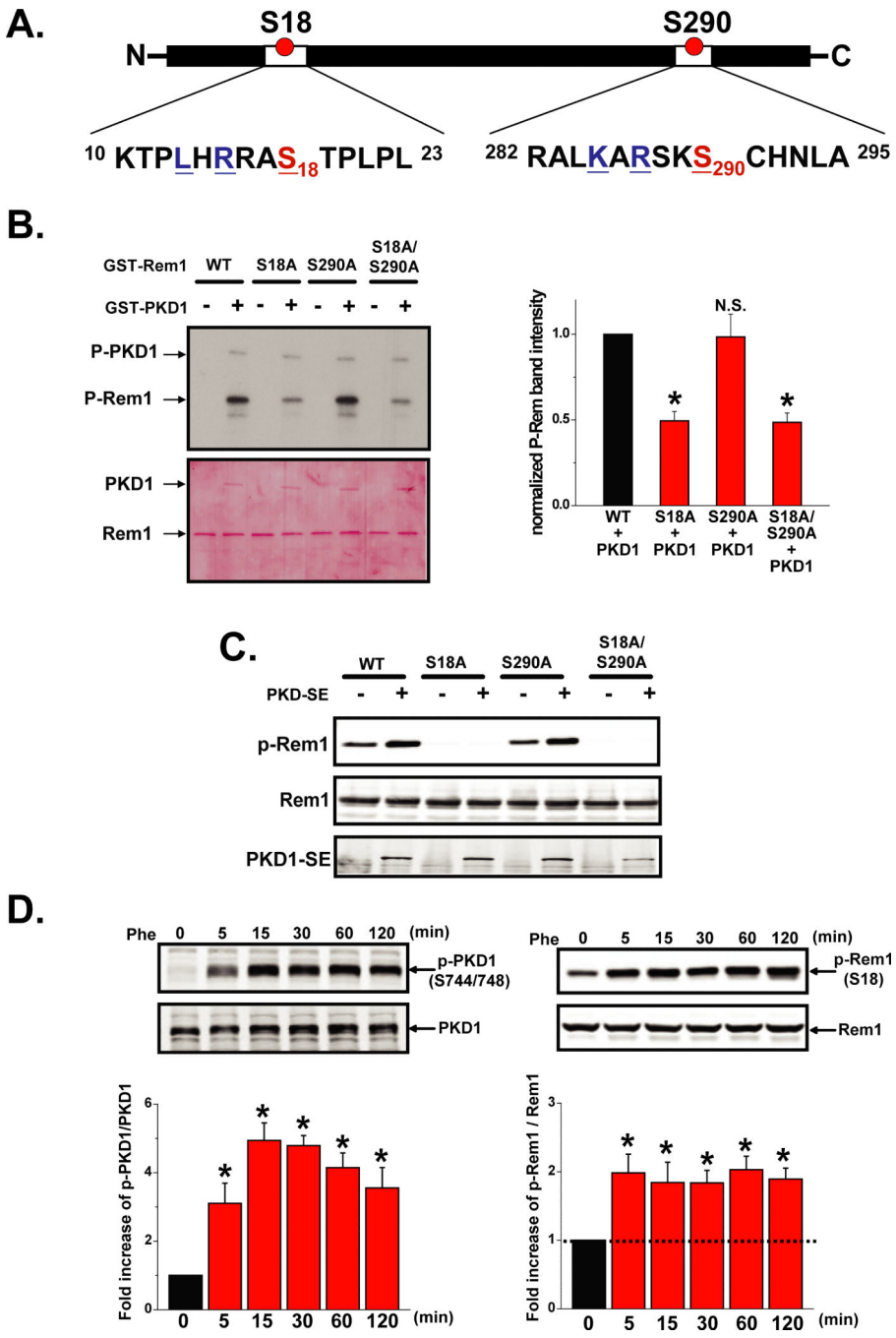

Figure 3. α_1-AR stimulation triggers PKD1-mediated phosphorylation of Rem1 at Ser18

A. Diagram highlighting two potential PKD motifs in Rem1. **B.** *In vitro* phosphorylation of Rem1 and mutant-Rem1 GST-fusion proteins (upper panel). Equal loading was verified by Ponceus S staining of membrane (lower panel). Bar graphs (right panel) show the summary data (n=3). **C.** Constitutive active PKD1 (PKDSE) phosphorylates Rem1-Ser18 in Hela cells. **D.** α_1-AR stimulation activates PKD1 and induces Rem1 phosphorylation at Ser18 in HEK293T cells (n=3).

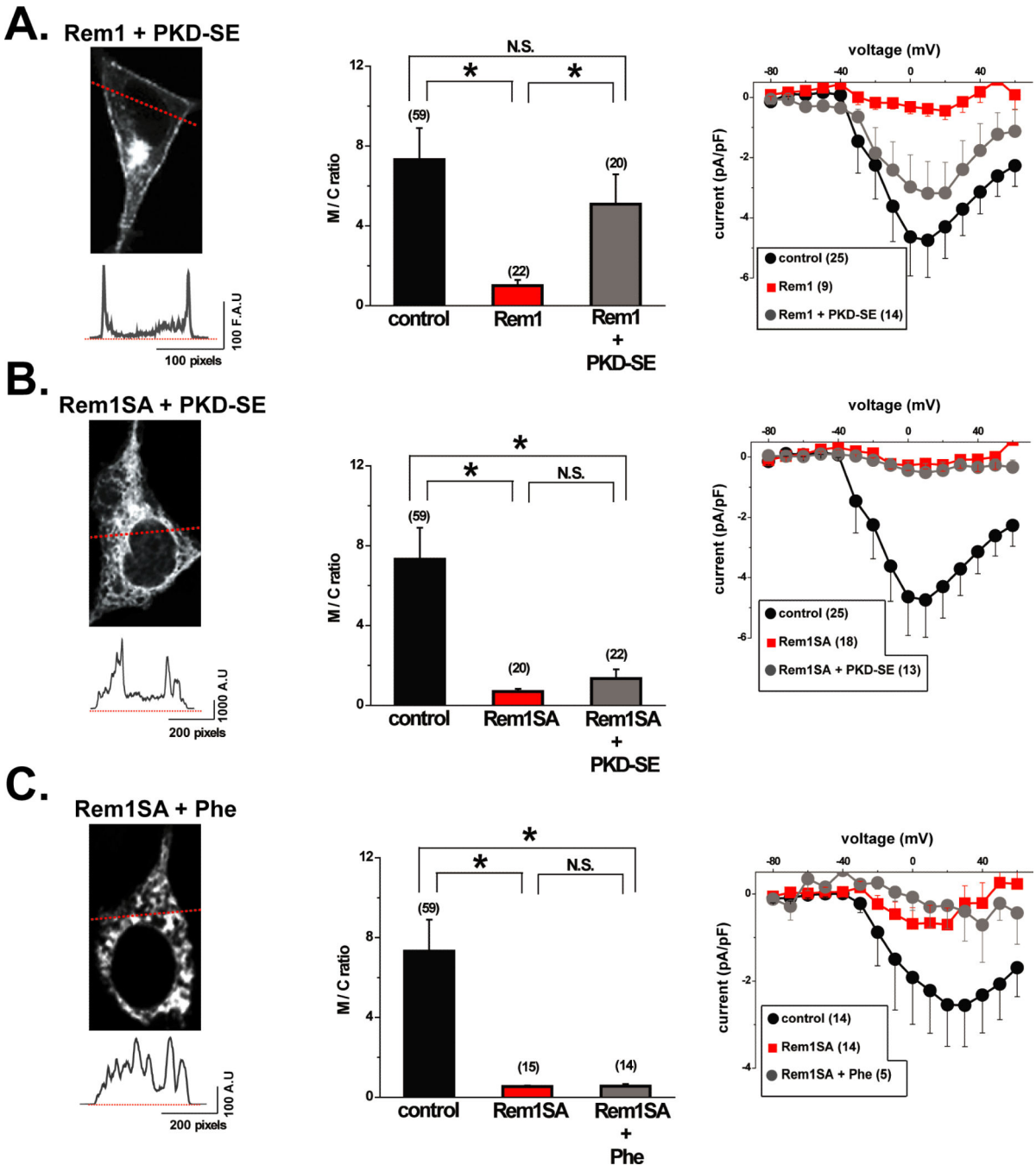

Figure 4. α_1-AR stimulation regulates VLCC surface membrane expression through PKD1-dependent phosphorylation of Rem1 at Ser18

A. Constitutively active PKD1 (PKD-SE) induces VLCC membrane expression in HEK293T cells co-transfected with Rem1. VLCC subunits and Rem1 were co-transfected with (gray) or without PKD-SE (red). Representative confocal image of cells transfected with VLCC, Rem1 and PKD-SE expression results in GFP-tagged Cav1.2 primarily localized in the surface membrane (left). M/C ratio of fluorescence intensity is shown compared with control (black, cells transfected with VLCC subunits) (middle). Current-voltage relationships were obtained from these 3 groups (right). **B.** Mutation of the PKD

phosphorylation site in Rem1 (S18 A) attenuated PKD1-induced VLCC expression at the plasma membrane. VLCC subunits and mutant Rem1-S18A were co-transfected with (grey) or without PKD-SE (red). Representative confocal image from a cell co-transfected with VLCC, Rem1-S18A and PKD-SE shows that GFP-CaV1.2 subunits were primarily localized within the cytosolic region of the cell (left). The M/C ratio of fluorescence intensity compared with control cells (black) (middle panel). Current-voltage relationships were obtained from these 3 groups (right). **C.** Expression of mutant Rem1-S18A blocked Phe-induced enhancement of Ca^{2+} channel expression in the plasma membrane. VLCC subunits, α_1-AR and mutant Rem1-S18A were co-transfected in HEK293T cells. Cells were treated with (grey) or without Phe (red) for 2 hours. Representative confocal image of cells transfected with VLCC subunits, α_1-AR and Rem1-S18A shows that GFP-α_{1C}-subunits were localized in the surface membrane after Phe stimulation (left). The M/C ratio of fluorescence intensity is shown compared with control cells (black) (middle). Current-voltage relationships were obtained from these 3 groups (right).

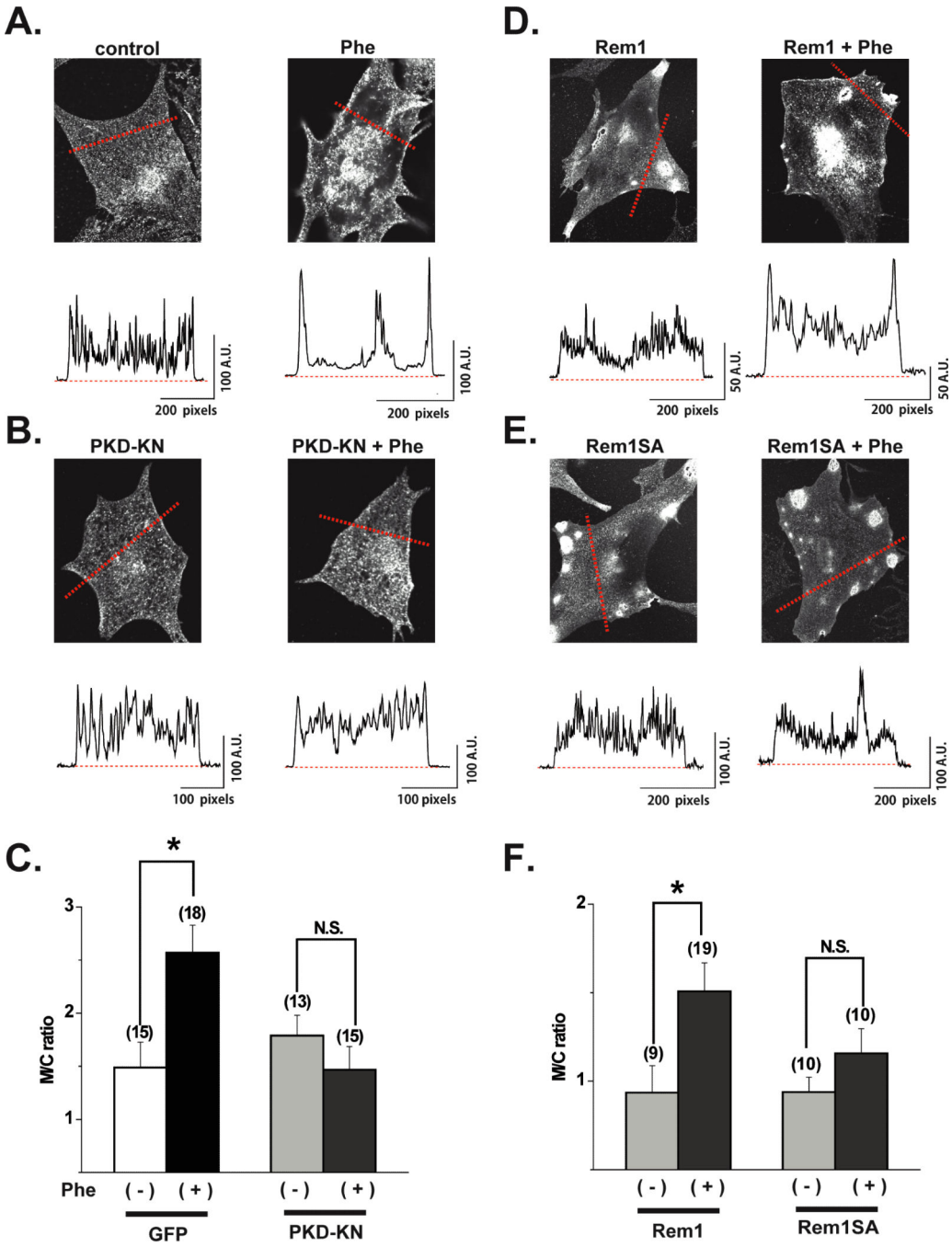

Figure 5. α_1-AR stimulation enhances VLCC membrane expression through PKD1-dependent phosphorylation of Rem1 at Ser18 in neonatal cardiomyocytes

A. Subcellular localization of Ca^{2+} channels in the absence (left) and presence (right) of α_1-AR stimulation (10 μM Phe for 2 hours) in native neonatal cardiomyocytes. Myocytes were fixed and stained with anti-$Ca_V1.2$ antibody. The profiles of immunofluorescence intensities are shown below with the cross-section indicated in the pictures above by the white dotted lines. **B.** Subcellular localization of Ca^{2+} channels in the absence (left) and presence (right) of α_1-AR stimulation (10 μM Phe for 2 hours) in native neonatal cardiomyocytes infected with adenovirus encoding GFP-tagged kinase-negative PKD1 (PKD-KN). **C.** Summary of

the M/C ratios of $Ca_V1.2$ immunofluorescence intensity in cardiomyocytes infected with either GFP or PKD-KN adenovirus. The number of the cells used for analysis is shown in parentheses. **D.** Subcellular localization of Ca^{2+} channels in the absence (left) and presence (right) of α_1-AR stimulation (10 μM Phe for 2 hours) in native neonatal cardiomyocytes infected with adenovirus encoding Myc-tagged WT-Rem1 (Rem1). **E.** Subcellular localization of Ca^{2+} channels in the absence (left) and presence (right) of α_1-AR stimulation (10 μM Phe for 2 hours) in native neonatal cardiomyocytes infected with adenovirus encording Myc-tagged Rem1(S18A) (Rem1SA). **F.** Summary of the M/C ratios of $Ca_V1.2$ immunofluorescence intensity in cardiomyocytes infected with either Rem1 or Rem1SA adenovirus.

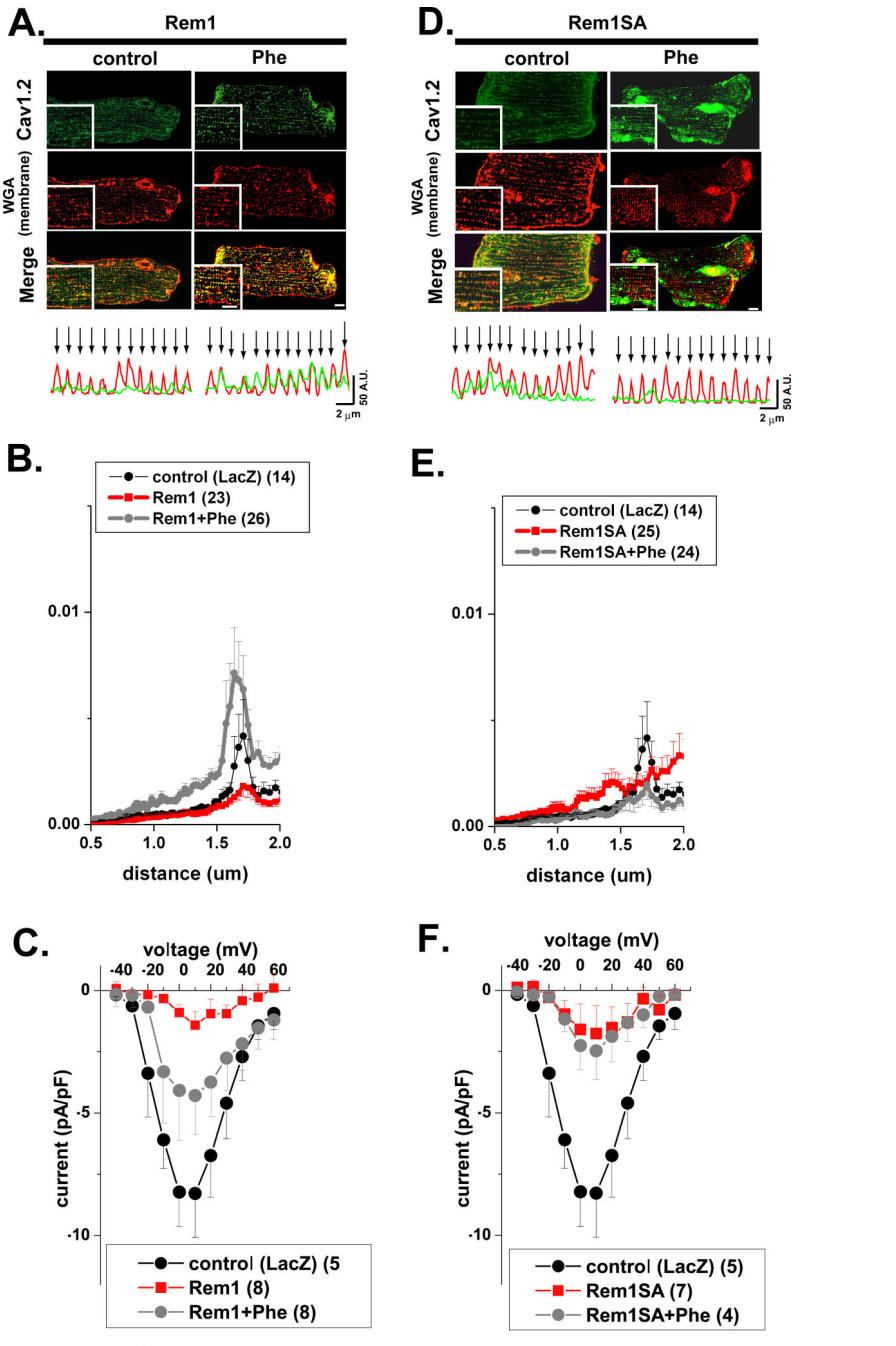

Figure 6. α_1-AR stimulation enhances VLCC expression at T-tubules through PKD1-dependent phosphorylation of Rem1-Ser18 in adult cardiomyocytes

A. Subcellular localization of VLCC in the absence (left) and presence (right) of α_1-AR stimulation (10 μmol/L Phe for 2 hours) in adult ventricular myocytes infected with Myc-tagged WT-Rem1 (Rem1). The averaged profiles of immunofluorescence intensities from $Ca_V1.2$ staining (green) and plasma membrane marker WGA (red) from inset windows except surface membrane are also shown at the bottom. **B.** Summary of FFT power spectrum retrieved from $Ca_V1.2$ staining images (characterized the power magnitude of the regular organization of T-tubule system) in the absence (red) and presence (grey) of α_1-AR

stimulation infected with WT-Rem1. The data from LacZ-infected cells is also shown as control (black). **C.** Effect of Rem1 expression and Phe stimulation on current-voltage relationship of I_{Ca}. **D.** Subcellular localization of VLCC in the absence (red) and presence (grey) of α_1-AR stimulation in cardiomyocytes infected with Rem1(S18A) (Rem1SA). **E.** Summary of FFT power spectrum retrieved from $Ca_V1.2$ staining images in the absence (left) and presence (right) of α_1-AR stimulation infected with Rem1SA. **F.** Effect of Rem1SA expression and Phe stimulation on current-voltage relationship of I_{Ca}.

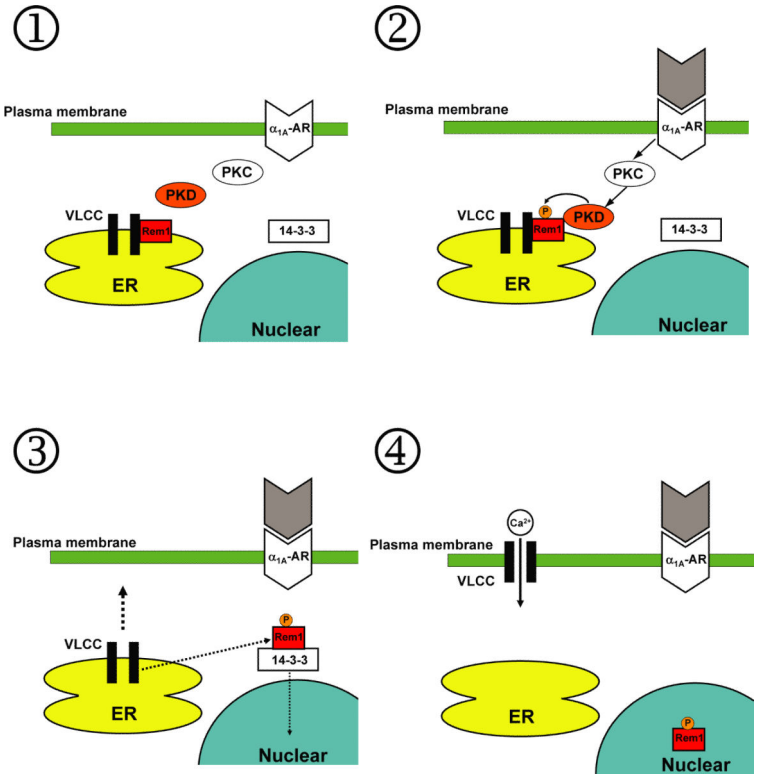

Figure 7. Proposed α_1-AR-PKD1-Rem1-14-3-3 mechanism for the regulation of VLCC membrane expression

1. Rem1 blocks VLCC membrane expression and inhibits VLCC activity by retaining VLCCs in ER. **2.** α_1-AR stimulation activates PKD1, which then directly phosphorylates Rem1-Ser18. **3.** Phosphorylation of Rem1-S18 increases binding to 14-3-3 and induces Rem1 translocation from cytosol to the nucleus. **4.** Rem1 nuclear translocation attenuates the inhibitory effect of Rem1 on VLCC expression, releasing the channel from the ER to traffic to the plasma membrane.